An Analytical Method for Failure Prediction of Composite Pinned Joints

Olanrewaju Aluko

***Abstract*— An analytical method for computing the stresses was developed to predict bearing strength of pinned loaded composite joints using the characteristic curve model. Unlike conventional method that involved bearing test and both tensile tests to failure of notched and notched plates, the characteristic length in compression and tension that defines the characteristic curve was evaluated from stress functions without experimental tests. Two different graphite/epoxy laminates were used in the analysis to evaluate the joint strength for different joint configurations. The available experimental data in literature was used to validate the obtained results and the method of analysis was confirmed adequate by the good agreement between the experimental data and the analytical results.**

***Index Terms*—Bearing, Experimental, Stress functions, Pinned loaded.**

I. Introduction

COMPOSITE materials offer the advantage of high specific strength and stiffness; in recent years they have been used extensively in aerospace structures, space vehicles and robotics structures. However, mechanically fastened joints that are needed for fitting component parts usually constitute a region of weakness that can lead to premature failure of structures. Based on the understanding that the engineering performance of a composite structure depends on its joints rather than the component members, the stresses and failure associated with mechanical joining of composites has received much attention. Mechanically fastened joints include bolted, riveted and pinned joints. These joints are susceptible to high stress concentrations which occur around and in the vicinity of the hole and are often the cause of unexpected failure in composite structures containing joints [1-16]. Therefore, adequate design of mechanical joint requires correct determination of the stresses, bearing strength and mode of failures of the joint. Wang et al.[3] investigated the possibility of changing the bolt and hole shapes from circular to elliptical in order to reduce bearing stress, and thereby increase the joint strength, especially when it is not possible to increase the hole diameter due to insufficient edge distance. Their analysis showed that the bearing stress at the joint hole can be significantly reduced by changing the bolt shape to elliptical. Chang et al. developed [11] characteristic length method for the failure analysis of composite joints and it is still currently used.

Manuscript submitted February 18, 2011.

Olanrewaju Aluko is with the University of Michigan-Flint, 303 E. Kearsley Street, Flint, MI 48502 USA (phone: 810-762-3181; fax: 810-766-6780; e-mail: aluko@ umflint.edu).

The conventional methods of determining characteristic length for failure analysis of composite joints usually involve bearing test and, tensile test of notched and unnotched plate to failure, which often leads to materials waste. In an attempt to prevent materials waste and thereby save cost, Kweon et al. [15] utilized the finite element method to determine the characteristic lengths for failure analysis of composite joints without characteristic length tests. The investigation showed how both compressive and tensile characteristic lengths can be numerically determined without bearing and tensile tests, respectively, and found the method to be very efficient in analyzing different joint configurations. The failure loads and modes based on numerically calculated characteristic lengths are also validated by the test results for composite joints with good agreement.

Based on the fact that a considerable amount of computational effort and time is often saved when an existing analytical solution is utilized in preference to any available finite element model, an analytical model for evaluating the characteristic lengths without tests is proposed in the present investigation. Thus an analytical method for computing the stresses in pinned loaded composite joints is presented based on Lekhnitskii's [5] complex stress functions, which satisfies the displacement boundary conditions along the hole contour. It was shown in this study that compressive and tensile characteristic length can be analytically determined without bearing test from stress functions based on the new definition [15] for characteristic length. The present study investigated the influence of joint configurations on the bearing strength. In the analysis, it was assumed that the pin is rigid and frictionless, with the diameter of the hole on the orthotropic plate equals to the diameter of the pin. Additionally, the contact boundary is assumed to span through half of the hole circumference.

In this study, the stresses obtained from stress functions are utilized to predict the bearing strength of pin loaded composite joints using Yamada-Sun failure criterion along the characteristic curve. The characteristic length in compression and tension obtained analytically without testing are utilized to construct the characteristic curve model.

II. Characteristic Length Methods

Several strength prediction methods for composite joints have been proposed, including stress concentration coefficient, damage zone model based on fracture energy and progressive failure analysis, and failure area index

ISBN: 978-988-19251-5-2
ISSN: 2078-0958 (Print); ISSN: 2078-0966 (Online)

(FAI). However, one of the most common and efficient methods of predicting the strength is the characteristic length method. This method was proposed by Whiney and Nuismer [1, 7], and it has been further developed by Chang et al. [11]. For this method, both the characteristics length in tension, R_t and compression, R_c must be determined by stress analysis associated with the results of bearing and tensile tests on notched and unnotched plates before employing an appropriate failure theory along the characteristic curve, r_c as shown in Figure 1. This characteristic curve which was first proposed by Chang et al. [11] can be expressed as

$$r_c = d + R_t + (R_t - R_c)cos\theta \quad (1)$$

where x and y are equal to $r_c cos\theta$ and $r_c sin\theta$ respectively.

By definition, the characteristic length (in tension or compression) is the distance from the edge of hole boundary over which the plate must be critically stressed to initiate sufficient flaw that can cause failure.

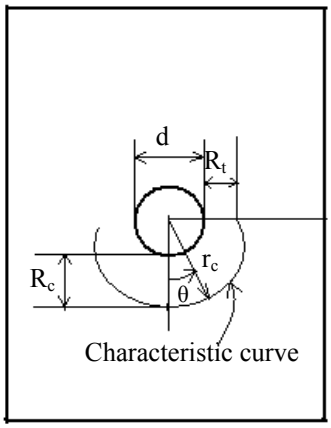

Fig. 1. Schematic Diagram for the Characteristic curve

This analytical method entails the determination of stress distributions within the plate and at the pin-plate interface. In order to demonstrate the practical application of characteristic length method, Whitney-Nuismer's point stress criterion [7] and Yamada failure criterion [12] are used to predict the joint's strength.

In this study, the CPL1 plate [15] with layers $[\pm45_3/90/\pm45_2/0_4/90/0_4//\pm45_2/90/\pm45_3]$ was utilized. The notation "±45" is used to represent a plain weave graphite/epoxy layer. The lamina thicknesses of the unidirectional and woven fabric layers are 0.114 mm and 0.198 mm, respectively. The unidirectional layers are from the USN125 graphite/epoxy prepreg by Hankook Fiber Glass. The DMS2288 graphite/epoxy woven fabrics are by Sunkyong. Another typical example utilized in this analysis is AS4/3502 graphite/epoxy laminate having the stacking sequence $[(0/\pm45/90/\bar{0})]_s$ and diameter 6.35 mm; lamina thickness h and width w, of 0.127 mm and 38.1 mm, respectively [4]. A typical example of the joint configuration of this pin loaded plate is shown in Figure 2. The material properties of the laminates and joint configurations are as given in Tables I and II. It should be noted that the 'rs' in joint identification codes WDrs shown in Tables II and III can be interpreted as w/d=rs.

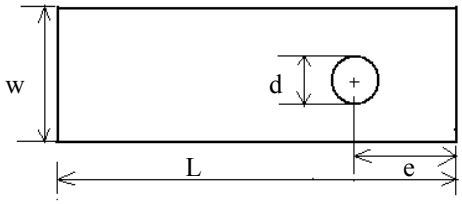

Fig. 2. The configurations of the joint

TABLE I
THE MATERIAL PROPERTIES OF COMPOSITE MATERIALS [4, 15]

Properties	Type of Material		
	USN 125	DMS 2288	AS4/3502
E_1 (GPa)	131	65	124.11
E_2 (GPa)	8.2	65	9.722
G_{12} (GPa)	4.5	3.6	3.744
υ_{12}	0.281	0.058	0.28
X_c (MPa)	1400	692.9	1406.60
X_t (MPa)	2000	959	1778.93
Y_c (MPa)	130	692.9	238.57
Y_t (MPa)	61	959	53.506
S_{12} (MPa)	70	65	102.05

TABLE II
GEOMETRIES OF COMPOSITE JOINTS [3, 15]

Plate	Joint ID	Hole-diameter, d mm	Width, w (mm)	Edge-distance, e mm	w/d	e/d
CPL1	WD20	9.53	19.00	13.40	2.0	1.4
	WD25	9.53	23.80	13.40	2.5	1.4
	WD28	9.53	26.80	13.40	2.8	1.4
	WD35	9.53	33.40	13.40	3.5	1.4
	WD40	9.53	38.00	13.40	4.0	1.4
AS4/ 3502	WD60	6.35	38.10	38.10	6.0	6.0

Compressive characteristic length

The conventional method of determining characteristic length for failure analysis of composite joints usually involves a bearing test. As stated earlier, for the characteristic length method of predicting joint strength, compressive characteristic length is an important parameter that must be determined. In this analysis, the no-bearing test method introduced by Kweon et al. [15] is employed, using analytical techniques for the determination of compressive characteristic length.

Although Whitney and Nuismer [19] suggested the characteristic length to be a material constant, several authors have shown that this value depends on specimen geometry [8,18]. To determine the characteristic length in compression, the approach proposed by Keweon [15] was used. This method utilizes an arbitrary applied load to compute the mean bearing stress defined by:

$$\sigma_{mb} = {}^{P_m}/_{bH} \quad (2)$$

where P_m is the applied load and H the laminate thickness. The compressive characteristic length R_c, as showed in Figure 2, is the distance from the front hole-edge to a point

ISBN: 978-988-19251-5-2
ISSN: 2078-0958 (Print); ISSN: 2078-0966 (Online)

where the local compressive stress by the arbitrarily applied load is the same as the mean bearing stress.

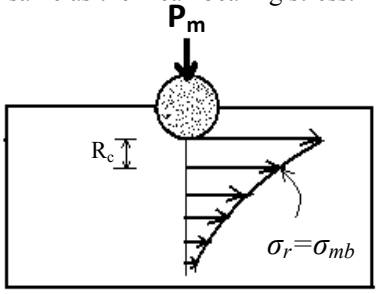

Fig. 2. Schematic diagram of the compressive characteristic length and normal stress distribution pattern

For the case where the plate is loaded as shown in Fig. 2, the stress functions can be expressed in the form [6]:

$$\emptyset_1(z_1) = Aln\varsigma_1 + \left({}^{1}/_{2D}\right)[(u_1q_2 - iv_1p_2)\varsigma_1^{-2} + (u_2q_2 - iv_2p_2)\,\varsigma_1^{-2}] \quad (3b)$$

$$\emptyset_2(z_2) = Bln\varsigma_2 + \left({}^{1}/_{2D}\right)[(u_1q_1 - iv_1p_1)\varsigma_2^{-2} + (u_2q_1 - iv_2p_1)\,\varsigma_2^{-2}] \quad (3a)$$

and the stresses in rectangular co-ordinate expressed as:

$$\sigma_x = 2Re\{\mu_1{}^2\emptyset_1'(z_1) + (\mu_2{}^2\emptyset_2'(z_2)\}$$
$$\tau_{xy} = -2Re\{(\mu_1\emptyset_1'(z_1) + \mu_2\emptyset_2'(z_2)\}$$
$$\sigma_y = 2Re\{\emptyset_1'(z_1) + \emptyset_2'(z_2)\} \quad (4)$$

where

$z_1=x+\mu_1 y$; $z_2=x+\mu_2 y$ and $\mu_1$and μ_2 are roots of characteristics equation

$$a_{11}\mu^4 + (2a_{12} + a_{66})\mu^2 + a_{22} = 0 \quad (5)$$

and a_{ij} are the laminate elastic compliance.

To demonstrate the applicability of this method for the case of analytical solution, arbitrary compressive loads P_m were used to evaluate the characteristic length in compression for the laminate CPL1 given in Table I. Figure 3 shows the mean bearing stresses and normal stress distributions from hole edge due to the applied loads P_m of magnitudes 10.3, 8 and 6 kN; and the corresponding characteristic length R_c=3.479 mm for the laminate with major diameter equal to 9.53 mm. It can be seen on Figure 3 that for the different magnitude of arbitrary load used in the analysis, the evaluated compressive characteristic length is 3. 479 mm. Similar analysis was also performed for laminate AS43502 shown in Table I and the result presented in Table III.

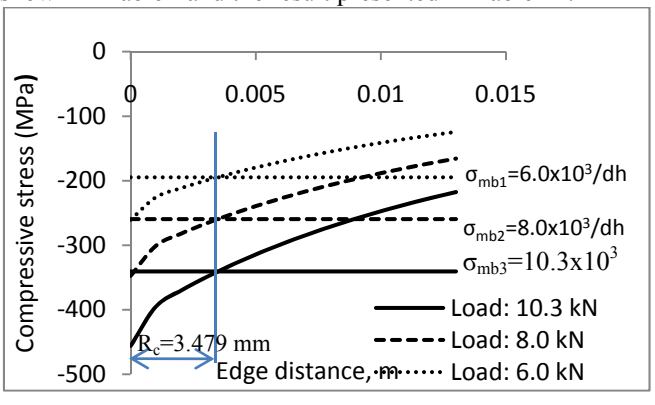

Fig. 3. Compressive characteristic length without bearing test for CPL1 laminate with WD=20

Tensile characteristic length

It has been stated that joints evaluation by characteristic length method also requires the determination of tensile characteristic length. Since the tensile strength of notched laminate and unnotched laminate must be known a priori, the conventional method involves the experimental tensile test to failure of notched and unnotched laminate. This method often leads to materials waste and a great deal of time is also required for testing. The present method utilized a new definition for tensile characteristic [15] to obtain characteristic length in tension. An arbitrarily tensile load Q_m is applied to the notched plate at infinity and the stress functions are used to obtain the stress distribution within the plate. Figure 4 shows the stress distribution of an infinite plate with a through-to-thickness hole subjected to distributed tensile loads per unit area, q_m at infinity. The tensile stress would be highest at the side edges of the hole, and decreases further away from the side edges of the hole as shown in this figure.

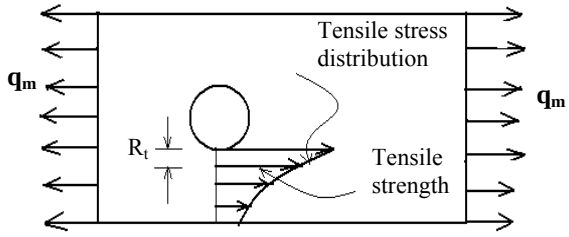

Fig. 4. Schematic diagram of the tensile characteristic length and stress distribution pattern

In this analysis, the Lekhnitskii's [5] complex stress functions are utilized to approximate the solution to the normal stress distribution σ_x (0,y) in an infinite orthotropic plate with an open hole loaded in tension. These functions can be expressed as

$$\emptyset_1(z_1) = -\frac{iq_m a}{2(\mu_1-\mu_2)}\frac{a-i\mu_1 a}{z_1+\sqrt{z_1^2-(a^2+\mu_1{}^2a^2)}} \quad (6)$$

$$\emptyset_2(z_2) = \frac{iq_m a}{2(\mu_1-\mu_2)}\frac{a-i\mu_2 a}{z_2+\sqrt{z_2^2-(a^2+\mu_2{}^2a^2)}} \quad (7)$$

where a is the radius of the hole and

$$\sigma_x = q + 2\mathrm{Re}\{\mu_1{}^2\emptyset_1'(z_1) + (\mu_2{}^2\emptyset_2'(z_2)\} \quad (8a)$$
$$\tau_{xy} = -2Re\{(\mu_1\emptyset_1'(z_1) + \mu_2\emptyset_2'(z_2)\} \quad (8b)$$
$$\sigma_y = 2Re\{\emptyset_1'(z_1) + \emptyset_2'(z_2)\} \quad (8c)$$

The point stress criterion [7] can be applied to Equation 8a to compute the tensile characteristic length at which failure analysis of the joint should be evaluated. The criterion defines the tensile characteristic length as the distance from the side-edge of the hole to a point where the local tensile stress by the arbitrarily applied load Q_m is the same as the mean tensile stress, defined by σ_{mt}. This can be expressed as

$$\sigma_x(0,y) = \sigma_{mt} \quad (9)$$

where,

$$y = r + R_t;\ Q_m = q_m(\mathrm{Wh}) \text{ and } \sigma_{mt} = \mathrm{Q_m}/(\mathrm{W}-\mathrm{d})\mathrm{h} \quad (10)$$

For conventional method, the value of tensile characteristic length can only be determined when the data for the notched

ISBN: 978-988-19251-5-2
ISSN: 2078-0958 (Print); ISSN: 2078-0966 (Online)

and unnotched laminate strength are known. However, the present analytical method, offers the advantage of computing the value of tensile characteristic length without experimental testing. To demonstrate the applicability of this method, the arbitrary loads Q_m of magnitude 12, 8 and 6 kN, respectively were used to compute the tensile characteristic length for graphite/epoxy plates with layers $[\pm45_3/90/\pm45_2/0_4/90/0_4//\pm45_2/90/\pm45_3]$ and a hole of 9.53 mm in diameter. The stress distribution and the calculated value of tensile characteristic length for w/d= 2.0 is shown in Figure 5. Similarly, this analysis is repeated for the CPL1 with various widths and also for $[(0/\pm45/90/\bar{0})]_s$ plate. The computed tensile characteristic lengths are shown in Table III.

TABLE III
THE COMPUTED CHARACTERISTIC LENGTHS FOR GRAPHITE/EPOXY PLATES

Plate	WD	R_c, mm	R_t, mm
CPL1	20	3.479	0.900
	25	3.479	1.470
	28	3.479	1.790
	35	3.479	2.490
	40	3.479	2.940
$[(0/\pm45/90/\bar{0})]_s$	60	0.810	3.272
$[(0/\pm45/0_3)]_s$	60	2.00	2.98

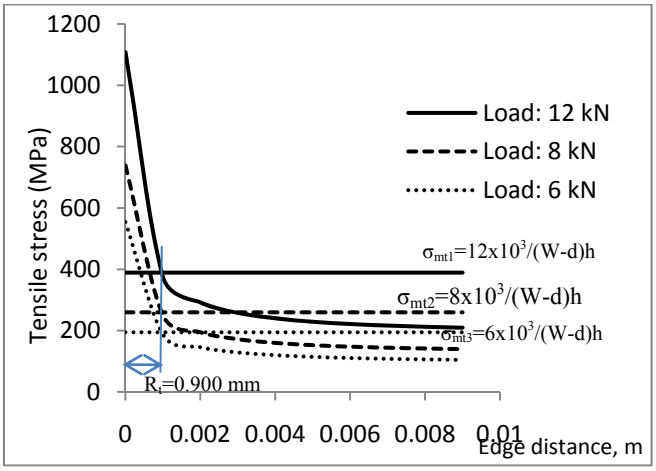

Fig. 5. Tensile characteristic length without experimental test for CPL1 laminate with WD=20

III. JOINT STRENGTH AND FAILURE ANALYSIS

The present study utilized a compact analytical technique that utilized the thickness of the plate as a parameter. The composite plate is considered to be homogeneous and infinite with a circular hole loaded by a rigid pin. In addition, the pin has the same diameter as the hole and the friction at the region of pin-plate contact is considered to affect the loading condition. The load F_r applied in x direction is assume to cause a displacement of c_o in its own direction and c_1 at the ends of contact boundary. It is assumed that the hole deforms into an ellipse under the action of the pin load F_r, which is also resisted by distributed load at infinity as shown in Figure 6. For the linear case of zero clearance, contact between the plate and the pin spans through half of the hole's circumference. Since the results from [3] have shown that the no-slip region within the contact boundary is zero degrees and this point is located at the point of symmetry, therefore the boundary conditions of the geometry shown in Figure 6 can be expressed as follow

Contact Region: $-\pi/2 \le\theta\le\pi/2$

$$u = c_o \text{ and } v = 0 \quad at\ \theta = 0 \tag{11}$$

$$u = c_1 \text{ and } v = 0 \quad \text{at } \theta = {}^{\pi}/_{2} \tag{12}$$

$$(c_o - u)\cos\theta = v\sin\theta \tag{13}$$

$$u = u_1\cos2\theta + u_2\cos4\theta \tag{15}$$

$$v = v_1\sin2\theta + v_2\sin4\theta \tag{16}$$

where u_1, u_2, v_1 and v_2 are the unknowns to determine from boundary conditions.

where u and v are the displacements along x and y axes respectively.

In this analysis, frictionless condition is assumed at the contact boundary and this condition can be expressed as

$$\tau_{r\theta} = 0 \tag{17}$$

No-contact region: $\pi/2 \le\theta\le3\pi/2$

The condition for the no-contact surface can be expressed as

$$\sigma_{rr} = 0 \tag{18}$$

$$\tau_{r\theta} = 0 \tag{19}$$

Similarly, using Equations 15 and 16 to also satisfy the above displacement boundary conditions, the unknown u_i and v_i can be expressed as

$$u_1 = {}^{(c_o - c_1)}/_{2}\ , u_2 = v_2 = {}^{(c_o + c_1)}/_{2} \text{ and } v_1 = {}^{(3co + c_1)}/_{2} \tag{20}$$

Lekhnitskii [5] has shown that if the known boundary displacement at the contour of the opening can be expressed in the form

$$u^* = \alpha_0 + \sum_{m=1}^{\infty}\{\alpha_m\sigma^m + \bar{\alpha}_m\sigma^{-m}\}$$

$$v^* = \beta_0 + \sum_{m=1}^{\infty}\{\beta_m\sigma^m + \bar{\beta}_m\sigma^{-m}\} \tag{21}$$

and the components of the resultant forces that cause the displacement are given, then the stress functions can be expressed by the following relations

$$\phi_1 = A\ln\varsigma_1 + \left[\bar{\alpha}_1 q_2 - \bar{\beta}_1 p_2 + \frac{1}{2}\omega(ibq_2 + ap_2)\right]\frac{1}{D\varsigma_1} + \frac{1}{D}\sum_{m=2}^{\infty}\{\bar{\alpha}_m q_2 - \bar{\beta}_m p_2\}\varsigma_1^{-m} \tag{22a}$$

$$\phi_2 = B\ln\varsigma_2 - \left[\bar{\alpha}_1 q_1 - \bar{\beta}_1 p_1 + \frac{1}{2}\omega(ibq_1 + ap_1)\right]\frac{1}{D\varsigma_2} - \frac{1}{D}\sum_{m=2}^{\infty}\{\bar{\alpha}_m q_1 - \bar{\beta}_m p_1\}\varsigma_2^{-m} \tag{22b}$$

In Equations 21 and 22, $\sigma = e^{i\theta}$ and ω=0. Bars represent conjugate values, α_m and β_m are known coefficients that depend on the load distribution at the opening edge, α_0, β_0 are arbitrary constants, D is p_1q_2-p_2q_1, and ζ_k is the mapping function given by

$$\varsigma_k = \frac{z_k \pm \sqrt{z_k^2 - \mu_k^2 a^2}}{a - i\mu_k a} \quad k = 1,2 \tag{23}$$

where μ_k (k = 1,2) are the roots of the characteristic Equation 5.

The sign of the square-root term in Equation 23 is chosen so that that magnitude of the mapping function is greater or equal to one; that is the domain of the plate is mapped onto the exterior of the unit circle. Additionally, the constants *A*

ISBN: 978-988-19251-5-2
ISSN: 2078-0958 (Print); ISSN: 2078-0966 (Online)

and B of Equation 22 can be obtained from the following relations [5]

$$A = \left({}^{P}/_{\pi Hi}\right)\ \left(\mu_1\bar{\mu}_1 + \mu_1\mu_2 + \mu_1\bar{\mu}_2 - \left({}^{a_{12}}/_{a_{22}}\right)\mu_1\mu_2\bar{\mu}_1\bar{\mu}_2\right)/ \left((\mu_1 - \bar{\mu}_1)(\mu_1 - \mu_2)(\mu_1 - \bar{\mu}_2)\right) \quad (24a)$$

$$B = \left({}^{P}/_{\pi Hi}\right)\ \left(\mu_2\bar{\mu}_2 + \mu_1\mu_2 + \mu_2\bar{\mu}_1 - \left({}^{a_{12}}/_{a_{22}}\right)\mu_1\mu_2\bar{\mu}_1\bar{\mu}_2\right)/ \left((\mu_2 - \bar{\mu}_2)(\mu_2 - \mu_1)(\mu_2 - \bar{\mu}_1)\right) \quad (24b)$$

where as previously indicated bars represent conjugate values, a_{ij} are the laminate elastic compliance and H is the thickness of the plate.

By expressing σ in Equation 21in terms of trigonometric function defined by

$$\cos n\theta = \frac{\sigma^n + \sigma^{-n}}{2};\ \sin n\theta = \frac{\sigma^n - \sigma^{-n}}{2i} \quad (25)$$

and comparing Equations 15 and 16 with 21, the stress functions of Equation 22 can be expressed as [19]

$$\emptyset_1(z_1) = A\ln\varsigma_1 + \left({}^{1}/_{4D}\right)[\left((c_o - c_1)q_2 - i(3co + c_1)p_2\right)\varsigma_1^{-2} + \left((c_o + c_1)q_2 - i(c_o + c_1)p_2\right)\varsigma_1^{-2}] \quad (26)$$

$$\emptyset_2(z_2) = B\ln\varsigma_2 - \left({}^{1}/_{4D}\right)[\left((c_o - c_1)q_1 - i(3co + c_1)p_1\right)\varsigma_2^{-2} - \left((c_o + c_1)q_1 - i(c_o + c_1)p_1\right)\varsigma_2^{-2}] \quad (27)$$

where

$$p_1 = a_{11}\mu_1{}^2 + a_{12} \text{ and } p_2 = a_{11}\mu_2{}^2 + a_{12} \quad (28a)$$

$$q_1 = a_{12}\mu_1 + {}^{a_{22}}/_{\mu_1} \text{ and } q_2 = a_{12}\mu_2 + {}^{a_{22}}/_{\mu_2} \quad (28b)$$

Additionally, the stresses in rectangular co-ordinates can be expressed as

$$\sigma_x = 2\mathrm{Re}\{\mu_1{}^2\emptyset_1'(z_1) + (\mu_2{}^2\emptyset_2'(z_2)\} \quad (29a)$$

$$\tau_{xy} = -2\mathrm{Re}\{(\mu_1\emptyset_1'(z_1) + \mu_2\emptyset_2'(z_2)\} \quad (29b)$$

$$\sigma_y = 2\mathrm{Re}\{\emptyset_1'(z_1) + \emptyset_2'(z_2)\} \quad (29c)$$

The stresses in rectangular co-ordinates can be transformed to polar co-ordinates using the transformation matrix

$$\begin{bmatrix} \cos^2\theta & \sin^2\theta & 2\sin\theta\cos\theta \\ \sin^2\theta & \cos^2\theta & -2\sin\theta\cos\theta \\ -\sin\theta\cos\theta & \sin\theta\cos\theta & \cos^2\theta - \sin^2\theta \end{bmatrix} \quad (30)$$

The prescribed displacements c_o and c_1 can be obtained by utilizing frictionless condition at the contact region within the hole boundary. Therefore at the end of contact boundary, we have

$$\tau_{r\theta} = 0 \qquad \text{at } \theta = \pm\pi/2 \quad (31)$$

and expressing Equation 17 in resultant form, it can be expressed as

$$\int_0^{\frac{\pi}{2}} \tau_{r\theta}\, r d\theta = 0 \quad (32)$$

Substituting the stresses into the equations above before solving the two equations simultaneously yields:

$$c_0 = gF_r(9n + k(10 + 21n) - 10\nu_{12})/4H\pi(k^2(5 + 13n + 3n^2) + k(12n^2 + n(7 - 13\nu_{12}) - 10\nu_{12}) + \nu_{12}(-7n + 5\nu_{12})) \quad (33)$$

$$c_1 = gF_r(k(-10 - 11n) - 19n + 10\nu_{12}/4H\pi(k^2(5 + 13n + 3n^2) + k(12n^2 + n(7 - 13\nu_{12}) - 10\nu_{12}) + \nu_{12}(-7n + 5\nu_{12})) \quad (34)$$

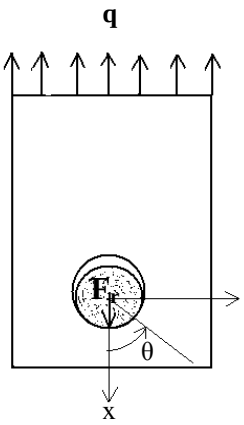

Figure 6. Schematic representation of composite joint under loading

where the parameters k, n and g are materials constant of the plate expressed as

$$k = -\mu_1\mu_2 = (E_1/E_2)^{1/2}$$
$$n = -i(\mu_1 + \mu_2) = [2(k - \nu_{12}) + E_1/G_{12}]^{1/2} \quad (35)$$
$$g = (1 - \nu_{12}\nu_{21})/E_2 + k/G_{12}$$

Utilizing Equations 33-35, the unknown coefficients u_i and v_i of the stress functions required to compute the stresses can be obtained from Equation 20 when the geometric parameters of the hole are known. The stress results computed from the above analytical method along the characteristic curve shown in Figure 1 were used in failure analysis to predict the joint strength. Additionally, Yamada-Sun failure criterion was used to test condition for first ply failure at any point along the characteristic curve. This criterion can be expressed as [12]

$$(\sigma_1/X)^2 + (\tau_{12}/S)^2 = e^2 \quad (36)$$

where σ_1 and τ_{12} are longitudinal compressive and shear stresses, respectively. X_c the ply longitudinal compressive strength and S the ply shear strength. In this model, failure is expected to occur when the value of e is either equal or greater than unity. The computer code that was used to test for the failure load was written in Mathematica. The failure of the joint can be characterized by three types of failure modes depending on the failure location, θ_f[11] namely:

$0° \le \theta_f \le 15°$: Bearing mode
$30° \le \theta_f \le 60°$: Shear − out mode
$75° \le \theta_f \le 90°$: Net − tension mode

Additionally, the concept of finite-width correction factor developed by Tan [9] was utilized to correct the infinite assumption of the plate. By definition, finite-width correction factor (FWC) is a scale factor which is applied to multiply the notched infinite plate solution to obtain the notched finite-plate result based on the assumption that the normal stress profile for a finite plate is identical to that for an infinite except for a FWC factor. This correction factor is given by the relationships

$$\frac{K_T^{\infty}}{K_T}\sigma_N^{\infty} = \sigma_N \quad (37)$$

where, σ_N and $\sigma_N{}^{\infty}$ denote the notched strength for finite and infinite plate, respectively, and $K_T/K_T{}^{\infty}$ is the FWC factor.

ISBN: 978-988-19251-5-2
ISSN: 2078-0958 (Print); ISSN: 2078-0966 (Online)

K_T and K_T^{∞} denote the stress concentration at the opening edge on the axis normal to the applied load for a finite plate and an infinite plate, respectively. This factor is expressed by the relationship [11]

$$\frac{K_T^{\infty}}{K_T} = \frac{\left[2-\left(\frac{2r}{W}\right)^2-\left(\frac{2r}{W}\right)^4\right]}{2} + \frac{\left(\frac{2r}{W}\right)^6\left(K_T^{\infty}-3\right)\left[1-\left(\frac{2r}{W}\right)\right]}{2} \quad (38)$$

$$K_T^{\infty} = 1 + \sqrt{\frac{2}{A_{22}}\left(\sqrt{(A_{11}A_{22})} - A_{12} + \frac{A_{11}A_{22}-A_{12}^2}{2A_{66}}\right)} \quad (39)$$

In Equation 39 A_{ij} denotes the effective laminate in plane stiffnesses.

IV. Results and Discussion

Two different Graphite/epoxy plates were used in this study to predict the strength of composite joints. Table IV data as displayed in Figure 7 shows the failure loads as compared with the experimental results from [15] for CPL1 joints with various ratios of width-to diameter (w/d). As mentioned before, the Yamada-Sun failure criteria were used to evaluate the failure of the joints. The results from this table showed that the predicted loads for different joint configurations are in agreement with experimental data. It is depicted on this table that the model slightly under predicts the failure load in most of the geometries except WD40 joints. Keweon et al. [9] stated that for each joint configuration, seven specimens were tested and they computed the coefficient of variation defined as standard deviation over the mean failure load to be 6.1 percent. Even though the range for the experimental failure load due to material variability cannot be computed from coefficient of variation, the present results still correlate well with experimental data and this shows that the present analytical model is adequate for the analysis of the joint strength. It can be seen from Table IV that failure load increases with increased width to diameter ratio. Also documented in Figure 8 is the failure loads for AS43502 joints with stacking sequence $[(0/\pm45/90/\bar{0})]_s$. There was no available experimental data for this joint but the present result was compared with result from Wang [4] as shown in this figure. The difference between the two results might be caused by the fact that Wang [4] used only tensile characteristic distance around the hole to evaluate the joint strength in lieu of characteristic curve model that requires both characteristic length in tension and compression.

TABLE IV
FAILURE LOADS AND MODES FOR CPL1 JOINTS

Joint ID	Failure Load, KN	
	Present	Exp
WD20	8.85	9.8
WD25	9.3	10.1
WD28	9.6	10.5
WD35	10.2	10.5
WD40	10.65	10.6

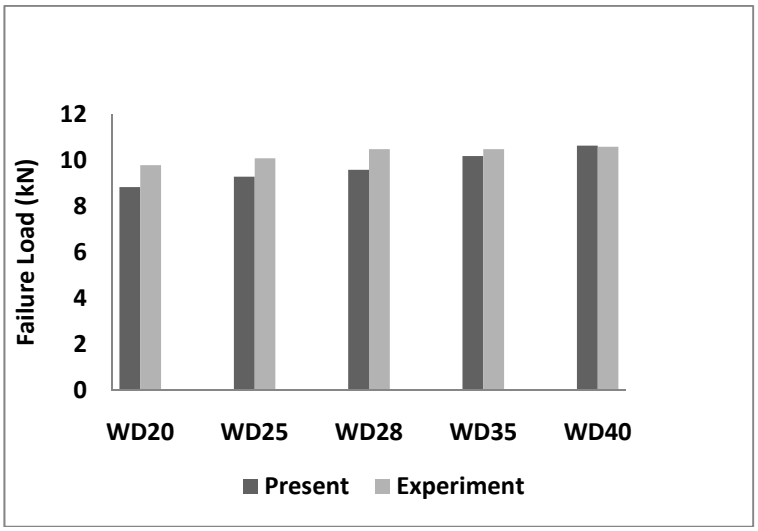

Fig. 7. Failure loads as compared with the experimental data from [15]

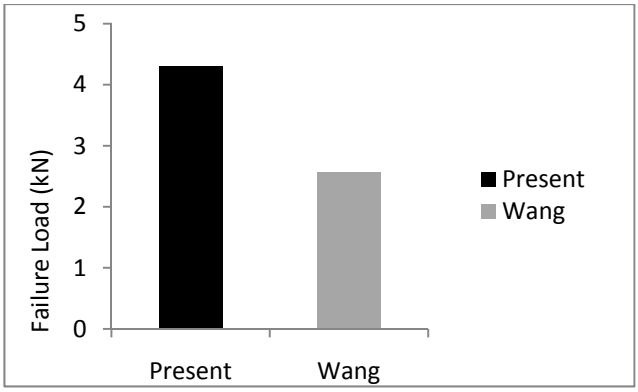

Fig. 8. Failure load for AS4/3502 joint with stacking sequence $[(0/\pm45/90/\bar{0})]_s$

V. Conclusion

Stress analysis was performed to predict the failure strength of pin loaded composite joints using Yamada-Sun failure criterion and the characteristic curve model. Unlike the conventional method that requires bearing test and tensile test of plates with and without hole, the characteristic dimensions that define the characteristic curve were obtained by stress analysis associated with no-bearing and also without tensile tests of the plate. The analytical result and available experimental data in literature for different laminated composite joint configurations were used to validate the present results. The method of analysis was proved adequate by the good agreement between the results found in literature and the present analytical results. The strength of the joints was also found to increase with width to diameter ratio.

Acknowledgment

The author acknowledges the financial support from the office of research, University of Michigan-Flint and the effort of Ms. Sue Koehler, for her time and patience in proof reading this manuscript.

REFERENCES

[1] R.J. Nuismer, "Application of the Average Stress Failure Criterion: Part II - Compression," Journal of Composite Materials, 13, 1979,pp. 49-60.
[2] H. A. Whitworth, M. Othieno, and O. Barton, "Failure analysis of Composite pin loaded Joints," composite Structures, 59, 2003, pp. 261-266.
[3] T. De Jong, "Stresses around pin-loaded holes in composite materials," Mechanics of composite materials recent advances. New York: Pergamon Press, 1982, pp. 339-353.
[4] J.T. Wang, C.G. Lotts, and D.D. Davis, "Analysis of bolt-loaded elliptical holes in laminated composite joints. Journal of reinforced plastics and composites," 12, 1993, pp. 128-138.
[5] S.G. Lekhnitskii, "Anisotropic Plates", Translated from the 2nd Russian edition by S.W. Tsai, and T. Chevron, Gordon and Breach, London, 1968.
[6] O. Aluko, "An Analytical Method to Determine Compressive Characteristic Length," District F Early Career ASME Journal, 2009, pp. 6.1-6.8.
[7] J.M. Whitney, and R.J. Nuismer, "Stress Fracture Criteria for Laminated Composites Containing stress Concentrations," Journal of Composite Materials," 10, 1974, pp. 253-265.
[8] J.M. Whitney, and R.J. Nuismer, "Uniaxial Failure of Composite Laminated Containing Stress Concentrations," Fracture Mechanics of Composite, ASTM STP, 1975, pp. 117-142.
[9] S.C. Tan, "Finite-width Correction Factor for Anisotropic Plates Containing Central Opening", Journal of Composite Materials," 22, 1988, pp. 1080-1097.
[10] S.C. Tan, "Laminated composites containing an opening elliptical II. Experiments and model modification," J. of composite Materials, 21, 1987, pp. 949-968.
[11] F.K. Chang, and R.A. Scott, "Strength of mechanically Fastened Composite joints," Journal of Composite Materials, 16, 1982, pp. 470-494.
[12] M.N. Nahas, "Survey of Failure and Post-Failure Theories of Laminated Fiber-Reinforced Composites," Journal of Composites Technology and Research, 8(4), 1986, pp.138-153.
[13] J. Choi and Y. Chun, "Failure Load Prediction of Mechanically Fastened Composite Joints," Journal of Composite Materials, 37(24), 2003, pp. 2163-2177.
[14] K. Zhang, and C.E.S. Ueng, "Stress Around a Pin Loaded Hole in Orthotropic Plates," Journal of Composite Materials, 18, 1984, pp. 432-446.
[15] J.,Ahn, H. Kweon, and J. Choi, "A new Method to determine the Characteristic Lengths of Composite Joints without Testing," Composite Structures, 66, 2004,pp. 305-315.
[16] H.J. Konish and J.M. Whitney, "Approximate Stresses in an Orthotropic Plate Containing a Circular Hole," Journal of Composite Materials, 9, 1975, pp. 157-166.
[17] L.J. Hart-Smith, "Mechanically Fastened Joints For Advanced composites phenomenological Considerations and Simple Analysis," Fibrous Composite in Structural Design, Plenum Press, 1980, pp. 543-574.
[18] R.F. Karlak, "Hole effects in a related series of symmetrical laminates," Proceedings 4th Joint ASM, Metallurgical Society of the American Mining Society, Metallurgical and Petroleum Engineers, Warrendale, PA, 1979.
[19] O. Aluko, "A compact analytical method for stress distribution in composite pinned joints" Ph.D. Thesis, Howard University, 2007.

ISBN: 978-988-19251-5-2
ISSN: 2078-0958 (Print); ISSN: 2078-0966 (Online)